Photocatalytic Degradation of Commercial Phoxim over La-Doped TiO2 Nanoparticles in Aqueous Suspension

ARTICLE *in* ENVIRONMENTAL SCIENCE AND TECHNOLOGY · APRIL 2009

Impact Factor: 5.33 · DOI: 10.1021/es802724q · Source: PubMed

5 AUTHORS, INCLUDING:

Tianyou Peng
Wuhan University
214 PUBLICATIONS **5,217** CITATIONS
SEE PROFILE

Hao Chen
Institute of engineering mechanics, China …
76 PUBLICATIONS **1,336** CITATIONS
SEE PROFILE

Environ. Sci. Technol. **2009,** *43,* 1540–1545

Photocatalytic Degradation of Commercial Phoxim over La-Doped TiO_2 Nanoparticles in Aqueous Suspension

KE DAI,[†] TIANYOU PENG,*[,†] HAO CHEN,*[,‡] JUAN LIU,[‡] AND LIN ZAN[†]

College of Chemistry and Molecular Science, Wuhan University, Wuhan 430072, P R China, and College of Science, Huazhong Agricultural University, Wuhan 430070, P R China

Received September 26, 2008. Revised manuscript received January 5, 2009. Accepted January 6, 2009.

Photocatalytic degradation of commercial phoxim emulsion in aqueous suspension was investigated by using La-doped mesoporous TiO_2 nanoparticles (m-TiO_2) as the photocatalyst under UV irradiation. Effects of La-doping level, calcination temperature, and additional amount of the photocatalyst on the photocatalytic degradation efficiency were investigated in detail. Experimental results indicate that 20 mg L^{-1} phoxim in 0.5 g L^{-1} La/m-TiO_2 suspension (the initial pH 4.43) can be decomposed as prolonging the irradiation time. Almost 100% phoxim was decomposed after 4 h irradiation according to the spectrophotometric analyses, whereas the mineralization rate of phoxim just reached ca. 80% as checked by ion chromatography (IC) analyses. The elimination of the organic solvent in the phoxim emulsion as well as the formation and decomposition of some degradation intermediates were observed by high-performance liquid chromatography−mass spectroscopy (HPLC-MS). On the basis of the analysis results on the photocatalytic degradation intermediates, two possible photocatalytic degradation pathways are proposed under the present experimental conditions, which reveal that both the hydrolysis and adsorption of phoxim under UV light irradiation play important roles during the photocatalytic degradation of phoxim.

Introduction

During recent decades, organophosphorus pesticides, a group of closely related pesticides that can affect the nervous system (*1*), have been widely used as an alternative to organochlorine compounds for pest control. These organic compounds are included in several priority lists of pollutants in many countries owing to their worldwide use, high toxicity for biotic systems, and probability of being discharged into the aquatic environment (*2*). Organophosphorus pesticide residues in agricultural products have been examined in two villages of Qianjiang, Hubei province, China. For example, the mean residue level of phoxim in vegetables was 89.9 μg kg^{-1} (*3*), which exceeds the national tolerance (GB 14868-94, China) (*4*). By this token, the development of innovative technologies for the degradation of phoxim into environmentally compatible compounds is of environmental interest. To the best of our knowledge, phoxim has never been selected as a contaminant in wastewater to investigate its behavior in the photocatalytic degradation (PCD) process. Furthermore, the organophosphorus pesticides used in most investigations have been purified rather than commercial ones (*5*). However, the commercial insecticide emulsion contains not only the pesticide but also the organic solvent, additive, and impurities, which could benefit the solubility and stability of the pesticide in water. Those coexisting compositions in emulsion can even cause additional complications in the PCD process due to possible reactions among the organic compounds mentioned above and their degradation byproducts (*6*). In addition, it is believed that there are formation and decomposition of a series of transient intermediates after the destruction of the main structure of the substrate during the PCD process (*7*) and the generated molecular fragments may have toxicological characteristics similar to or higher than its parent compound, which makes it obligatory to identify those intermediates (*8*).

TiO_2 nanoparticles, as an effective catalyst, have attracted attention in the research on PCD of organic pollutants. However, the fast recombination of the photogenerated electron−hole pairs on the surfaces or in the lattices of TiO_2 hindered the extensive application of the PCD technique (*9*). Since the photoactivity of TiO_2 depends strongly on the separation efficiency of the electron−hole pairs and its optical absorption property, TiO_2 can be improved by doping with impurities such as metals, metal ions, and semiconductor oxides, which could effectively eliminate the recombination of the photogenerated electron−hole pairs during the photocatalytic reaction (*10*). For example, it is reported that lanthanum (La) doping could efficiently stabilize the mesostructure of TiO_2 with crystallized walls and improve its photoactivity (*11*−*13*). Moreover, incorporation of lanthanide ions into TiO_2 matrix could also promote the chemical adsorption of the organic substrates on the photocatalyst surfaces, which also benefits the improvement of its photocatalytic efficiency (*9, 12, 14*).

La-doped TiO_2 nanoparticles with mesostructures (La/m-TiO_2) have been fabricated in our group and shown much better photoactivity than that of undoped ones and the commercial photocatalyst P25 (Degussa, Germany) due to its large surface area, highly crystallized mesoporous wall, and more active sites for concentrating the substrate (*13*). Herein, those La/m-TiO_2 nanoparticles with mesostructures were employed to investigate the effects of photoreaction conditions on the PCD efficiency of phoxim in commercial emulsion. Under the optimal photoreaction conditions, the mineralization products and photodegradation intermediates were examined by ion chromatography (IC) and high-performance liquid chromatography−mass spectroscopy (HPLC-MS), respectively. Then, the possible PCD pathways of phoxim were proposed.

Experimental Section

Chemicals and Materials. A commercial emulsion containing 40% w/w phoxim, 8% additive (Code Name Nongru 0201-B), and unspecified organic solvent (Sanonda Corporation, Hubei, China) was used to simulate contamination caused by an organophosphate insecticide in water. A phoxim standard (CAS No. 14816-18-3) was purchased from AccuStandard, Inc. (New Haven, CT). Preparation and characterization of the La/m-TiO_2 nanoparticles were conducted according to our previous publication (*13*). It is notewothy

* Address correspondence to either author. Tel: +86-27-8721-8474; fax: +86-27-6875-4067; e-mail: typeng@whu.edu.cn (T.Y.P.); hchenhao@mail.hzau.edu.cn (H.C.).

[†] Wuhan University.

[‡] Huazhong Agricultural University.

10.1021/es802724q CCC: $40.75
Published on Web 01/22/2009

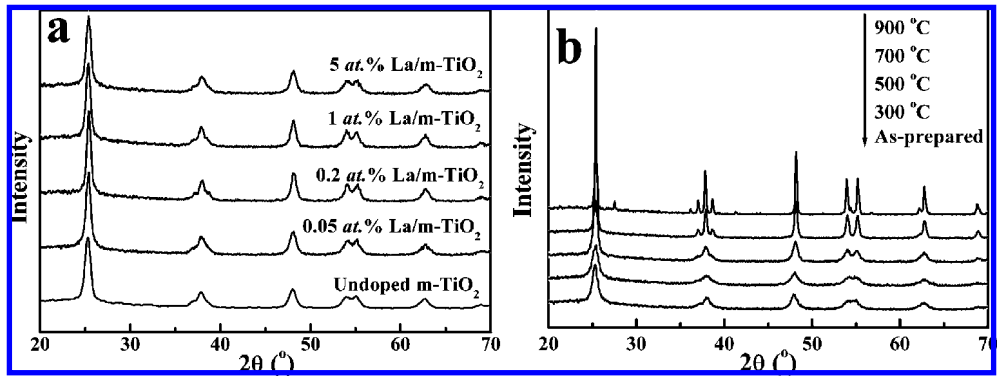

FIGURE 1. XRD patterns of the La-doped m-TiO_2 nanoparticles with (a) different doping levels and calcination at 500 °C; (b) 1 at.% La-doping and calcination at different temperatures.

that the molar ratio of $Ti(SO_4)_2$:$La(NO_3)_3$ was adjusted to obtain TiO_2 nanoparticles with different La-doping levels, and then the as-synthesized La/m-TiO_2 nanoparticles were calcined at different temperatures.

Photocatalytic Degradation Experiment. Photocatalytic reactions were performed in a PCD system described previously (*15*). Prior to irradiation, the pH value of the suspension was adjusted with HNO_3 or NaOH solutions. 0.5 g L^{-1} photocatalyst (1.0 at.% La/m-TiO_2 after calcination at 700 °C), 20 mg L^{-1} phoxim, initial pH 4.43, were used throughout the course of the investigation unless otherwise stated. A UV−vis spectrophotometer (Nicolet 300 evolution) was used for the determination of UV absorbance at 285 nm. The mineralized end-products (NO_2^-, NO_3^-, PO_4^{3-}, and SO_4^{2-}) in the filtrate produced during PCD of phoxim were analyzed by using a Dionex ICS-1000 ionic chromatography (Dionex, U.S.) equipped with an isocratic pump and a DS-6 conductivity detector. The eluent was 9 mmol L^{-1} Na_2CO_3 at a flow rate of 1.5 mL min^{-1}. The sample injection volume was 25 μL.

The PCD intermediates of phoxim produced from different irradiation periods under the optimal photoreaction conditions were analyzed through an Agilent 1100 HPLC-MS system (Agilent, U.S.) equipped with a Zorbax SB-C18 column (150 mm × 2.1 mm). The eluent was water/methanol (30/70, v/v) solution at a flow rate of 0.25 mL min^{-1}. A 2 μL sample was injected by using an autosampling device. The UV detector was operated at 285 nm. MS and MS^2 analyses in the positive mode were performed on 1100 MSD ion trap mass spectrometer equipped with an ESI ion source. The flow rate of the high-purity nitrogen (heater temperature 300 °C) was maintained at 7 L min^{-1}.

Computer Simulation. As reported by Zhu et al. (*16*), the optimal geometry conformation and the lowest energy of phoxim molecule were obtained at PM3 level by choosing a charge of 0 and a spin of 1. By calculating the values of the point charge and bond length, we can predict the adsorption sites on m-TiO_2 nanoparticles and the weak position of phoxim molecule in the initial photodegradation reaction. All above calculations were carried out by using Hyperchem 5.0.

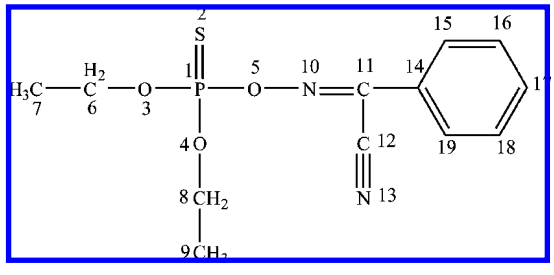

Results and Discussion

Crystal Phase Composition of La/m-TiO_2 Nanoparticles. The X-ray diffraction patterns of the m-TiO_2 nanoparticles calcined at 500 °C with different La-doping levels are shown in Figure 1a. All samples have a similar XRD pattern dominated by anatase phase. The relative intensity of the (101) diffraction peak for anatase first increases while enhancing the La-doping level from 0 to 1.0 at.% and then decreases with further enhancing to 5.0 at.%. These results suggest that moderate La-doping benefits the crystallization of anatase, whereas superfluous La-doping probably inhibits the phase transformation from amorphous to anatase of TiO_2 in the mesoporous wall, leading to a higher thermal stability (*12, 13*). Moreover, La-doping can efficiently improve the stability of mesostructures and enhance the specific surface area in comparison with the undoped one as shown in our previous publication (*13*).

Figure 1b shows the powder XRD patterns of 1.0 at.% La/m-TiO_2 after calcination at different temperatures. As can be seen, only peaks of anatase phase become stronger and sharper, indicating the improved crystallinity of anatase upon enhancing the calcination temperature from 80 to 700 °C (*ref.* Table S1 in the Supporting Information (SI)). Even after calcination at 900 °C for 2 h, the XRD pattern shows that the main crystal phases are still anatase, accompanied by appearance of a very small peak corresponding to the rutile phase. In a word, the enhanced thermal stabilities of anatase phase and the mesostructures of La-doped sample can be attributed to the La-doping and the existence of large amount of mesopores between the nanocrystallite wall (*17, 18*). The HRTEM image and EDX spectrum of 5.0 at.% La/m-TiO_2 are provided in Figures S1 and S2. Further information on the La/m-TiO_2 can be found in our previous publication (*13*).

Photolysis of Phoxim Solution. In aqueous solution, phoxim shows its maximum UV absorption peak at 285 nm, and the calibration curve based on the Beer−Lambert's law was used to determine the concentration of phoxim aqueous solution. Blank experiments demonstrated that the reduction of absorbance at 285 nm of the phoxim solution (pH = 6.11) was about 13% after 4 h irradiation in the absence of photocatalyst, which could be attributed to the photolysis of phoxim under UV irradiation considering the hydrolysis of phoxim can be neglected (the half-life of phoxim in aqueous solution (pH = 7) is 700 h (*19*)). To verify the photolysis reaction, UV-irradiated phoxim solutions were examined by IC. Figure S3 shows ion chromatograms of the inorganic products resulting from the photolysis of phoxim solutions after 2 and 4 h UV irradiation. None of the inorganic ions (PO_4^{3-}, SO_4^{2-}, NO_3^-, NO_2^-) was found except 0.028 mg L^{-1} SO_4^{2-} (t_R = 7.6 min) in the 4 h irradiated phoxim solution, which is equal to 4.5% mineralization rate of 20 mg L^{-1} phoxim solution. Since the blank experiments demonstrated that the

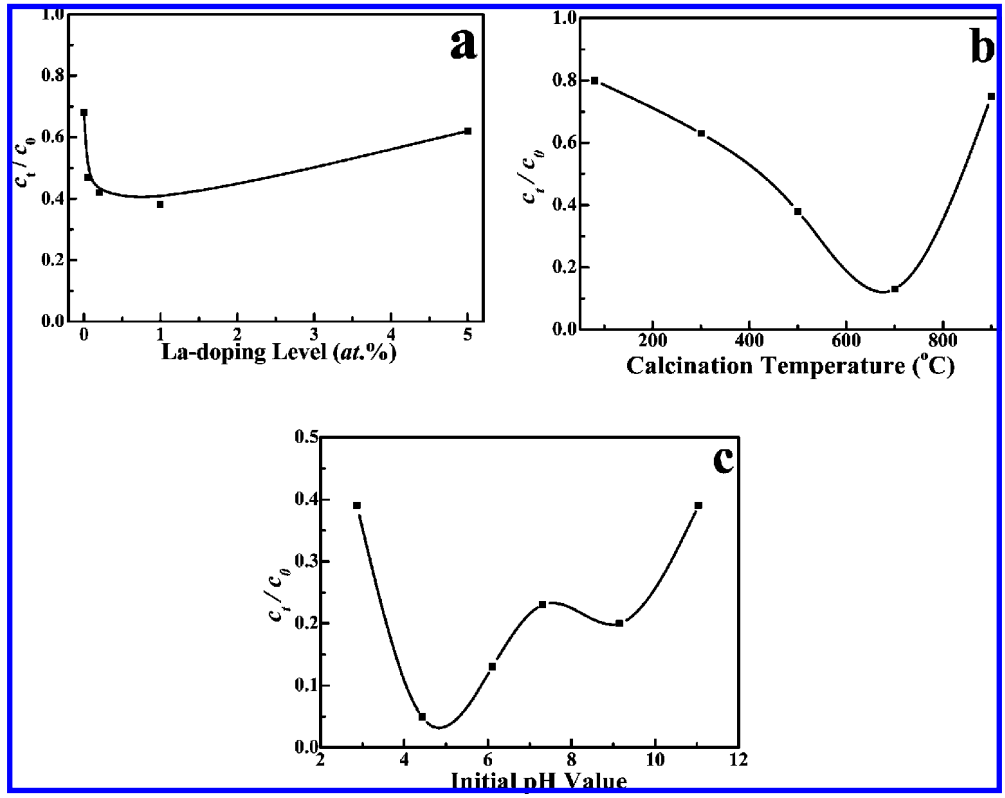

FIGURE 2. Effect of the La-doping level (a), calcination temperature (b), and initial pH value (c) on the photodegradation efficiency of phoxim in La-doped m-TiO_2 suspension.

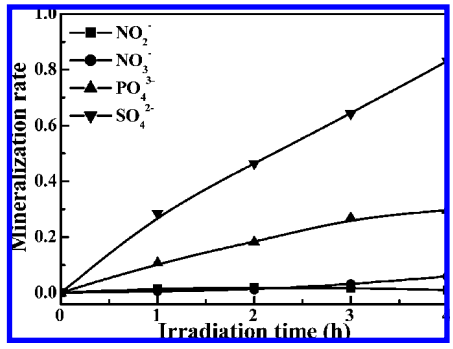

FIGURE 3. Evolution of inorganic anions during the photocatalytic degradation of phoxim under the optimal experimental conditions (20 mg L^{-1} phoxim, initial pH 4.43, 0.5 g L^{-1} 1.0 at.% La-doped m-TiO_2 after calcination at 700 °C).

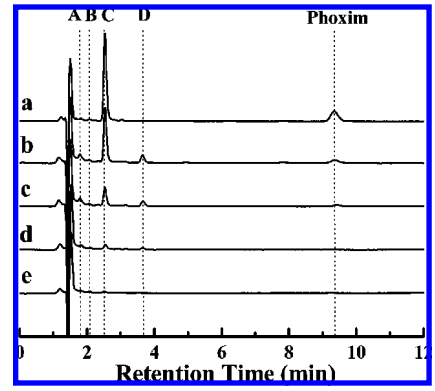

FIGURE 4. HPLC profiles of the phoxim solutions after different irradiation times: (a) 0 h, (b) 1 h, (c) 2 h, (d) 3 h, and (e) 4 h.

reduction of absorbance at 285 nm of the phoxim solution was about 13% after 4 h irradiation, we can presume that the photolysis of phoxim solution under UV irradiation did not lead to the complete mineralization but to the generation of some intermediates, which will be further discussed below.

Optimization of Photocatalytic Degradation Conditions. A set of PCD experiments after 3 h UV irradiation was carried out in an aqueous suspension containing 20 mg L^{-1} phoxim and 0.5 g L^{-1} La/m-TiO_2 with different La-doping levels (0, 0.05, 0.2, 1.0, and 5.0 at.%). As can be seen from Figure 2a, the PCD efficiency for phoxim increases initially with enhancing the La-doping level from 0 to 1 at.%, and then decreases while further enhancing to 5.0 at.%. In other words, appropriate La-doping can efficiently enhance the photoactivity of TiO_2 nanoparticles and the 1.0 at.% La/m-TiO_2 shows the best performance in the present experimental condition. This phenomenon can be rationalized by the mechanism of photoactivity enhancement due to the La-doping, which has also been reported by Li and co-workers (*12*). Appropriate La-doping level in TiO_2 can enhance the separation efficiency of the electron−hole pairs by entering the crystal lattices of TiO_2 (*ref.* Table S2), and then improve the photocatalytic performance. However, excessive La-doping will be presented as oxide on the surfaces of TiO_2, which acts as the recombination centers and then decreases the photoactivity of TiO_2 (*20*).

Figure 2b presents the effect of calcination temperature of 1.0 at.% La/m-TiO_2 on the PCD efficiency of phoxim after 3 h UV irradiation. As can be seen, the PCD efficiency increases upon enhancing the temperature from 80 to 700 °C, and then decreases while enhancing to 900 °C. The sample calcined at 700 °C exhibits the best photoactivity among the tested samples, indicating that 700 °C is the most appropriate calcination temperature, which was used thereafter. This result can be explained by the combined influences of the crystallinity, crystal phase, and surface area of La/m-TiO_2 on its photocatalytic activity (*21, 22*).

TABLE 1. Point Charge and Bond Length on Atoms of the Phoxim at the PM3 Level

atom	point charge	bond	bond length	atom	point charge	bond	bond length
P1	1.8810	P1−S2	1.9171	C11	0.1018	C11−C12	1.4341
S2	−0.6028	P1−O3	1.6824	C12	−0.1268	C11−C14	1.4764
O3	−0.6076	P1−O4	1.6838	N13	−0.0168	C12−N13	1.1589
O4	−0.5980	P1−O5	1.7422	C14	−0.0711	C14−C15	1.3984
O5	−0.5226	O3−C6	1.4042	C15	−0.0768	C14−C19	1.3979
C6	0.1412	O4−C8	1.4044	C16	−0.1061	C15−C16	1.3902
C7	−0.1264	O5−N10	1.3621	C17	−0.0802	C16−C17	1.3908
C8	0.1310	C6−C7	1.5199	C18	−0.1010	C17−C18	1.3914
C9	−0.1302	C8−C9	1.5200	C19	−0.0741	C18−C19	1.3895
N10	0.0251	N10−C11	1.3058				

The effect of initial pH value on the PCD efficiency of phoxim was investigated after 3 h UV irradiation. As shown in Figure 2c, the best PCD efficiency was obtained under pH 4.43, which is the optimal pH condition under the present experiment conditions and was used thereafter. The zero point of charge (pH_{ZPC}) of La-doped TiO_2 nanoparticles was reported to be 5.3−5.7 (*21*), so that the surface is negatively or positively charged at higher or lower than this pH, respectively. To predict the details of the adsorption mode of phoxim on the TiO_2 surfaces, point charges of all individual atoms in phoxim molecule were calculated by means of PM3 method, which has been reported by Zhu et al. (*16*) and Horikoshi et al. (*23*). The calculated results are summarized in Table 1, which demonstrates that there are only five atoms carrying positive charge among all 19 atoms in phoxim molecule. Therefore, under the lower pH value (pH 4.43) than the pH_{ZPC}, the photocatalyst surface is positively charged and is propitious to the adsorption of phoxim and then to the PCD efficiency. Furthermore, sulfur atom (S2) among the four atoms possessing large negative charge is presumed to be the linking point to the surface of the catalyst due to the following considerations: (1) although atoms O3, O4, and O5 also carried a large negative charge, steric hindrance restrains them from becoming the linking point; (2) bond length of P1−S2 is the longest one among all bonds in phoxim molecule, which facilitates the adsorption owing to the long distance between the both positively charged P1 and La/m-TiO_2. In other words, under the present pH value, phoxim molecules can be adsorbed on the La/m-TiO_2 surfaces through the S2−H−O−Ti bond due to the following equilibrium: $Ti{-}OH + H^+ \leftrightarrow TiOH_2^+$ (*16*). The effect of the addition amount of photocatalyst on the PCD efficiency was also optimized. As shown in Figure S4, the best efficiency was obtained with 0.5 g L^{-1} 1 at.% La/m-TiO_2 in the aqueous suspension.

Evolution of Inorganic Anions Derived from Photocatalytic Degradation of Phoxim. The theoretical maximum concentration of NO_2^- (6.17 mg L^{-1}), NO_3^- (8.32 mg L^{-1}), PO_4^{3-} (6.38 mg L^{-1}), and SO_4^{2-} (6.44 mg L^{-1}) was calculated assuming a 100% mineralization rate of the phoxim according to eq 1:

$$C_{12}H_{15}O_3PSN_2 + O_2 \rightarrow CO_2 + H_3PO_4 + H_2SO_4 + HNO_3 + H_2O \quad (1)$$

The mineralization ratios of the final products were obtained through quantitative analysis of the degraded solutions by IC. Evolutions of various inorganic ions (PO_4^{3-}, SO_4^{2-}, NO_3^-, NO_2^-) as a function of irradiation time from 0 to 4 h are shown in Figure 3. After 4 h UV irradiation, the mineralization ratios of S, P, and N were 80.0, 27.0, and 5.0%, respectively. These phenomena can be rationalized by the differences in the bond energies of chemical bonds linked to these atoms. As shown in Table 1, bond P1−S2 possesses the longest bond length in the phoxim molecule, which suggests the P−S bond is the most fragile site during the PCD reaction. In contrast, C12−N13 and C11−N10 possess the shortest bond length, implying that they are hard to break. Under the present experimental condition, the total mineralization ratio of nitrate and nitrite did not reach the expected stoichiometric value, which is probably attributed to the generation of some intermediates during the PCD process. In addition, it must be noted that nitrite was not detected in our reaction system, which is important since the concentration of NO_2^- in drinking water is strictly limited (0.01 mg L^{-1}).

Determination of Photodegradation Intermediates. Figure 4 reports the HPLC profiles recorded at 285 nm corresponding to the degradation products of the commercial phoxim after 0, 1, 2, 3, and 4 h UV irradiation. By analyzing the samples through HPLC-MS, the significant peaks produced at various degradation times are labeled as mentioned below. As can be seen from Figure 4a, the peak at $t_R = 9.3$ min (m/z 298) corresponds to phoxim, which is proved by the fragments and rupture pathways of phoxim molecule in the ESI-MS profile (Figure S5). Although no initial carbon has been mineralized, there is another relatively strong peak at $t_R = 2.5$ min (m/z 198, denoted as compound C) with a large abundance. Considering the large abundance of the compound C in the solution without UV irradiation, it can be attributed to the organic solvent in the commercial phoxim emulsion. However, the peak of the organic solvent C disappeared after 4 h irradiation, suggesting that this organic solvent can be readily photocatalytically decomposed in the La/m-TiO_2 suspension and there was no additional complication caused by the reaction between this organic solvent and the degradation byproducts of phoxim. After 1 h irradiation, three new peaks are clearly observed except for the three peaks corresponding to the mobile phase ($t_R = 1.5$ min), compound C ($t_R = 2.5$ min), and phoxim ($t_R = 9.3$ min) as shown in Figure 4b. The three new peaks at $t_R = 1.8$ min (m/z 170), 2.0 min (m/z 184), and 3.6 min (m/z 282) are denoted as intermediates A, B, and D, respectively. As can be observed from Figure 4c, many peaks of the colored intermediates are still present after 2 h irradiation, but the phoxim exhibits a much smaller peak in comparison with Figure 4a. Except for the organic solvent C and phoxim, the other peaks increase first and subsequently decrease without formation of new derivatives upon prolonging the irradiation time, suggesting that the formation and transformation, as well as the chromophore breaking, of those intermediates could proceed simultaneously. It is worthy to notice that all these chromatographic peaks exhibit retention times shorter than that of the phoxim, implying that no intermediate with larger molecular weight or polarity than that of phoxim was formed, which excludes the possibility of the polymerization reaction in the present system (*6*).

Plots of the peak intensities recorded in the HPLC profiles for the detected intermediates and phoxim against the irradiation time are depicted in Figure S6. It is clearly shown that the formation and subsequent decomposition of these

SCHEME 1. Proposed photocatalytic degradation pathways for phoxim in La-doped m-TiO_2 suspension.

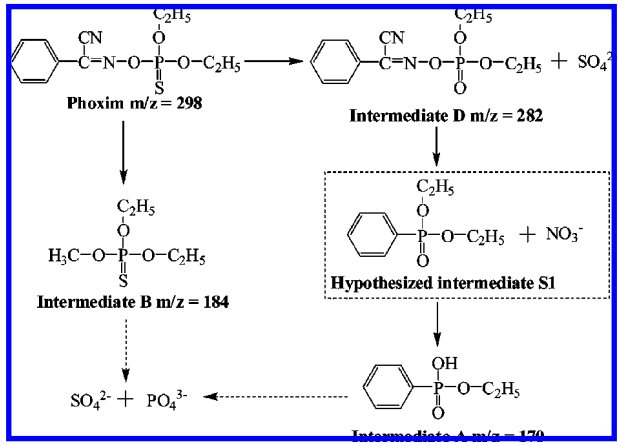

intermediates occurred accompanying with the abatement of phoxim and all three intermediates reached their maximum concentration after approximately 1 h UV irradiation. It is noteworthy that, unlike compound A or D, the decrease of compound B is quite slow after 1 h UV irradiation, which could be related with its structure and formation mechanism.

Investigation on Photodegradation Mechanism of Phoxim. In the present work, three types of intermediates possessing chromophore were detected; their UV−vis spectra obtained by diode array detection are shown in Figure S7. It is observed that the intermediates A, B, and D have quite different spectral characteristics, corresponding λ_{max} are 227, 232, and 284 nm, respectively. These experimental facts indicate that intermediates A, B, and D have different structures. Furthermore, the spectrum of intermediate B has no peak at ca. 277 nm, which can be attributed to the $\pi \rightarrow \pi^*$ transition located in the aromatic rings, implying that the intermediates B probably do not possess the benzene ring (*15*). In contrast, the spectra of both intermediate A and D show a peak at ca. 285 nm, indicating that these two intermediates may have molecular structure analogous to the phoxim. Especially, the structures of intermediate D and phoxim could have small difference since their spectra are very similar.

With the observation from total ion chromatogram and mass spectra profile of the individual intermediate obtained by MS and MS^2 analysis, the possible structures of the intermediates A, B, and D can be proposed, and then the possible degradation pathways can be concluded. Scheme 1 tentatively suggests the PCD pathways for phoxim in the La/m-TiO_2 suspension, which is focused only on those reaction pathways that are consistent with the present experimental facts. In order to mechanistically rationalize the formation of intermediate A from the phoxim photodegradation, the presence of the intermediate S1 (indicated in dashed pane in Scheme 1) is simply hypothesized.

As can be seen, the intermediates A, B, and D are identified to be monoethyl phenylphosphonate, *O,O*-diethyl *O*-methyl phosphorothioate, and *O,O*-diethyl *O*-(alpha-cyano benzylideneamino) phosphonate, respectively. Among those intermediates, compound B can be attributed to the methylated product of the hydrolysate from phoxim. As it is reported that thiophosphate would undergo hydrolysis at the ester group while irradiated by UV light in aqueous solution (*24*), the hydrolysis of phoxim would give birth to the *O,O*-diethyl phosphonothioate radical, which would subsequently reacted with $\cdot OCH_3$ (*25*) and finally generate the intermediate B. However, the hydrolysate of phoxim was not observed in our study, which can be attributed to its lower stability than that of intermediate B. This presumption is also consistent with the slow decrease of intermediate B after 1 h UV irradiation (Figure S6).

On the basis of previous observations on the reaction behavior of phoxim in the presence of La/m-TiO_2 and UV irradiation, two possible photodegradation pathways can be proposed: the first one yields substitution of the S atom by O atom, whereas the second one starts with the hydrolysis under UV irradiation, namely, breaking the ester bond between the diethyl ester of thiophosphoric acid and benzimidoyl cyanide moiety of the molecule. The second photodegradation pathway accounted for the phenomenon that the photolysis of phoxim under UV irradiation did not lead to complete mineralization. This finding suggests the importance of examining the photolysis product of organic pollutants while studying their PCD pathways under UV irradiation.

In general, for the TiO_2 suspension under UV irradiation, the oxidative activity of TiO_2 particles is mostly attributed to the species formed through reactions initiated by the photogenerated electron (e^-)−hole (h^+) pairs, such as hydroxyl radicals, hydroperoxyl and other peroxyl radicals, valence-band holes in TiO_2, and hydrogen peroxide (*26*). Although the general steps in the PCD process of the organic pollutants in TiO_2 suspension are no longer questioned, the subsequent details of the degradation pathway remain rather controversial (*27*). Watanabe and co-workers (*28*) found that OH radicals in the solution bulk can principally attack the aromatic ring of Rhodamine B, leading to hydroxylation. In contrast, at the photocatalyst/solution interfaces, dealkylation is the dominant degradation pathway. Moreover, the positive holes are considered as the major oxidative species at a low pH level whereas the hydroxyl radicals are considered as the predominant species at a neutral or high pH level (*29*).

After the S substitution, the first pathway becomes similar to the second one, i.e., the disruption takes place of the ester bond between the diethyl ester of the phosphoric acid and benzimidoyl cyanide moiety, which gives rise to the formation of the hypothesized intermediate S1. By a further action of OH radicals, the hypothesized intermediate S1 would transform into intermediate A due to the hydroxylation reaction. The PCD pathways of phoxim favor the cleavage of P1═S2 and P1−O5 bonds, which is in accordance with their long bond lengths as observed from the results of computer simulation (Table 1). Furthermore, phoxim molecules were adsorbed on La/m-TiO_2 surfaces through S2−H−O−Ti bond, which also makes the S2 atom easily to be attacked.

In the present system, there is only one hydroxylated intermediate found, i.e., the intermediate A, indicating the hydroxylation is not the dominant pathway in the initial degradation step. These phenomena can be rationalized by the substrate adsorption on the surfaces of semiconductors, which plays an important role in the PCD process (*30*). As mentioned above, under the present relatively low pH value (pH 4.43), the positively charged photocatalyst surface is propitious to the adsorption of phoxim. It is reported that at the moment of excitation, tight binding of substrate to the photocatalyst favors the electron transfer during the PCD reaction (*31*). Therefore, on the basis of the analysis above, the electron transfer mechanism is also expected in the phoxim photodegradation under the present conditions, especially for the initial steps. Then, after the tight binding (S2−H−O−Ti bond) between substrate and photocatalyst was destroyed, the hydroxylation dominated the degradation pathway and then led to the generation of intermediate A.

Acknowledgments

This work was supported by the National "863" Foundation of China (2006AA03Z344), Natural Science Foundation of China (20573078), and Program for New Century Excellent Talents in University (NCET-07-0637), China. We thank Dr.

E.N. Yang of Huazhong Agricultural University for the HPLC-MS analysis.

Supporting Information Available

The preparation process, TEM image, and EDX spectrum of 5 at.% La/m-TiO_2 nanoparticles, fwhm values of the XRD diffraction peaks at $2\theta = 25.28°$ for La/m-TiO_2 nanoparticles, cell parameters *a* and *c* of m-TiO_2 and La/m-TiO_2 nanoparticles, ion chromatograms of phoxim solutions after 2 and 4 h UV irradiation, effect of the addition amount of 1 at.% La/m-TiO_2 on the photocatalytic degradation efficiency of phoxim, fragments of phoxim molecule in ESI-MS profile, evolution profile of phoxim and its intermediates identified by HPLC analysis, UV−vis spectra of the phoxim and its degradation intermediates A, B, D. This material is available free of charge via the Internet at http://pubs.acs.org.

Literature Cited

(1) U.S. EPA. *Summary of the Risks and Uses of Organophosphate Methyl Parathion*; 2000; http://www.epa.gov/pesticides/op/methylparathion/methylsum.htm (accessed May 9, 2008).

(2) Tang, Y. F.; Wang, Y. X.; Cai, H. S.; Merkel, B. J. Extraction and concentration of micro OPs from water sample by activated carbon fiber. *Res. Environ. Sci* **2004**, *26*, 46–48; in Chinese.

(3) Agricultural Bureau of Qiangjiang, Hubei, China. http://www.qjagri.gov.cn/index.asp(in Chinese) (accessed April 14, 2008).

(4) Ye, J. M.; He, Y. B.; Tao, C. J. Introduction to the national standard on pesticide residues of China. *Pest. Sci Admin.* **2000**, *21*, 20–23; in Chinese.

(5) Chen, S. F.; Cao, G. Y. Photocatalytic degradation of organophosphorus pesticides using floating photocatalyst $TiO_2 \cdot SiO_2$/beads by sunlight. *Sol. Energy* **2005**, *79*, 1–9.

(6) Dai, K.; Peng, T. Y.; Chen, H.; Zhang, R. X.; Zhang, Y. X. Photocatalytic degradation and mineralization of commercial methamidophos in aqueous titania suspension. *Environ. Sci. Technol.* **2008**, *42*, 1505–1510.

(7) Devipriya, S.; Yesodharan, S. Photocatalytic degradation of pesticide contaminents in water. *Sol. Energy Mater. Sol. Cells* **2005**, *86*, 309–348.

(8) Arnold, S. M.; Hickey, W. J.; Harris, R. F. Degradation of atrazine by Fenton's reagent: condition optimization and product quantification. *Environ. Sci. Technol.* **1995**, *29*, 2083–2089.

(9) Uzunova-Bujnova, M.; Todorovska, R.; Dimitrov, D.; Todorovsky, D. Lanthanide-doped titanium dioxide layers as photocatalysts. *Appl. Surf. Sci.* **2008**, *254*, 7296–7302.

(10) Chen, X. B.; Mao, S. S. Titanium dioxide nanomaterials: synthesis, properties, modifications, and applications. *Chem. Rev.* **2007**, *107*, 2891–2959.

(11) Yuan, S.; Sheng, Q. R.; Zhang, J. L.; Yamashita, H.; He, D. N. Synthesis of thermally stable mesoporous TiO_2 and investigation of its photocatalytic activity. *Microporous Mesoporous Mater.* **2008**, *110*, 501–507.

(12) Li, F. B.; Li, X. Z.; Hou, M. F. Photocatalytic degradation of 2-mercaptobenzothiazole in aqueous La^{3+}-TiO_2 suspension for odor control. *Appl. Catal., B* **2004**, *48*, 185–194.

(13) Peng, T. Y.; Zhao, D.; Song, H. B.; Yan, C. H. Preparation of lanthana-doped titania nanoparticles with anatase mesoporous walls and high photocatalytic activity. *J. Mol. Catal., A* **2005**, *238*, 119–126.

(14) Xu, A. W.; Gao, Y.; Liu, H. Q. The preparation, characterization, and their photocatalytic activities of rare-rarth-doped TiO_2 nanoparticles. *J. Catal.* **2002**, *207*, 151–157.

(15) Dai, K.; Chen, H.; Peng, T. Y.; Ke, D. N.; Yi, H. B. Photocatalytic degradation of methyl orange in aqueous suspension of mesoporous titania nanoparticles. *Chemosphere* **2007**, *69*, 1361–1367.

(16) Zhu, X.; Yuan, C.; Bao, Y.; Yang, J.; Wu, Y. Photocatalytic degradation of pesticide pyridaben on TiO_2 particles. *J. Mol. Catal., A* **2005**, *229*, 95–105.

(17) Sibu, C. P.; S. Kumar, R.; Mukundan, P.; Warrier, K. G. K. Structural modifications and associated properties of lanthanum oxide doped sol-gel nanosized titanium oxide. *Chem. Mater.* **2002**, *14*, 2876–2881.

(18) Gopalan, R.; Lin, Y. S. Evolution of pore and phase structure of sol-gel derived lanthana doped titania at high temperatures. *Ind. Eng. Chem. Res.* **1995**, *34*, 1189–1195.

(19) Vinopal, J. H.; Fukuto, T. R. Selective toxicity of phoxim (phenylglyoxylonitrile oxime *O, O*-diethyl phosphorothioate). *Pest. Biochem. Physiol.* **1971**, *1*, 44–60.

(20) Zhao, D.; Peng, T. Y.; Liu, M.; Lu, L. L.; Cai, P. Fabrication, characterization and photocatalytic activity of Gd^{3+}-doped titania nanoparticles with mesostructure. *Microporous Mesoporous Mater.* **2008**, *114*, 166–174.

(21) Parida, K. M.; Sahu, N. Visible light induced photocatalytic activity of rare earth titania nanocomposites. *J. Mol. Catal., A* **2008**, *287*, 151–158.

(22) Kim, H. R.; Lee, T. G.; Shul, Y. G. Photoluminescence of La/Ti mixed oxides prepared using sol-gel process and their pCBA photodecomposition. *J. Photochem. Photobiol., A* **2007**, *185*, 156–160.

(23) Horikoshi, S.; Serpone, N.; Yoshizawa, S.; Knowland, J.; Hidaka, H. Photocatalyzed degradation of polymers in aqueous semiconductor suspensions. IV theoretical and experimental examination of the photooxidative mineralization of constituent bases in nucleic acids at titania/water interfaces. *J. Photochem. Photobiol., A* **1999**, *120*, 63–74.

(24) Murdock, L. L.; Hopkins, T. L. Insecticidal *O,O*-dialkyl anticholinesterase, and hydrolytic properties of S-aryl phosphorothiolates in relation to structure. *J. Agric. Food Chem.* **1968**, *16*, 954–958.

(25) Xu, Z. G.; Jing, C. Y.; Li, F. S.; Meng, X. G. Mechanisms of photocatalytical degradation of monomethylarsonic and dimethylarsinic acids using nanocrystalline titanium dioxide. *Environ. Sci. Technol.* **2008**, *42*, 2349–2354.

(26) Li, X.; Cubbage, J. W.; Tetzlaff, T. A.; Jenks, W. S. Photocatalytic degradation of 4-chlorophenol. 1. the hydroquinone pathway. *J. Org. Chem.* **1999**, *64*, 8509–8524.

(27) Chen, C.; Pei, P.; Ji, H.; Ma, W.; Zhao, J. Photocatalysis by titanium dioxide and polyoxometalate/TiO_2 cocatalysts. Intermediates and mechanistic study. *Environ. Sci. Technol.* **2004**, *38*, 329–337.

(28) Watanabe, T.; Takizawa, T.; Honda, K. Photocatalysis through excitation of adsorbates. 1. highly efficient N-deethylation of rhodamine B adsorbed to cadmium sulfide. *J. Phys. Chem-US* **1977**, *81*, 1845–1851.

(29) Hu, C.; Yu, J. C.; Hao, Z.; Wong, P. K. Effects of acidity and inorganic ions on the photocatalytic degradation of different azo dyes. *Appl. Catal., B* **2003**, *46*, 35–47.

(30) Stylidi, M.; Kondarides, D. I.; Verykios, X. E. Visible light-induced photocatalytic degradation of Acid Orange 7 in aqueous TiO_2 suspensions. *Appl. Catal., B* **2004**, *47*, 189–201.

(31) Li, X.; Cubbage, J. W.; Jenks, W. S. Variation in the chemistry of the TiO_2-mediated degradation of hydroxy- and methoxybenzenes: electron transfer and $HO^{\bullet}_{ads}$ initiated chemistry. *J. Photochem. Photobiol., A* **2001**, *143*, 69–85.

ES802724Q